Supporting Information Appendix

Thiophene antibacterials that allosterically stabilize DNA-cleavage complexes with DNA gyrase

Pan F. Chan,[1†]* Thomas Germe,[2†] Benjamin D. Bax,[3†] Jianzhong Huang,[1†] Reema K. Thalji, [1†] Eric Bacqué,[4] Anna Checchia,[5] Dongzhao Chen,[1] Haifeng Cui,[1] Xiao Ding,[1] Karen Ingraham,[1] Lynn McCloskey, [1] Kaushik Raha,[1] Velupillai Srikannathasan,[3] Anthony Maxwell,[2] and Robert A. Stavenger[1]*

Correspondence to: pan.2.chan@gsk.com or robert.a.stavenger@gsk.com

Affiliations:
[1]Antibacterial Discovery Performance Unit, Infectious Diseases Therapy Area Unit, GlaxoSmithKline, 1250 Collegeville Rd., Collegeville, Pennsylvania, PA 19426, USA.
[2]Deptartment of Biological Chemistry, John Innes Centre, Norwich Research Park, Norwich NR4 7UH, UK.
[3]Platform Technology and Science, GlaxoSmithKline, Medicines Research Centre, Gunnels Wood Road, Stevenage, Hertfordshire, SG1 2NY, UK.
[4]Sanofi R&D, TSU Infectious Diseases, 1541 Avenue Marcel Mérieux, 69280, Marcy L'Etoile, France.
[5]Aptuit Center of Drug Discovery and Development, Via A. Fleming, 4, 37135, Verona, Italy.
*Corresponding author. E-mail: pan.2.chan@gsk.com (PFC) or robert.a.stavenger@gsk.com (RAS).
[†]These authors contributed equally to this work.
‡ Current address: Department of Chemistry, University of York, York YO10 5DD, UK.
§ Current address: Frontage Laboratories, Inc. 700 Pennsylvania Dr, Exton, PA 19341, USA.
¶ Current address: Data Sciences, Janssen Pharmaceuticals, Spring House, PA 19477, USA.
# Current address: Structural Genomics Consortium, Old Road Campus Research Building, Roosevelt Drive, University of Oxford, Oxford, OX3 7DQ, UK.

Supporting Materials and Methods

Synthesis of inhibitors. General. All reagents and solvents were purchased from commercial suppliers and used as received. Compound **1** was prepared according to a previously reported procedure (1). ^{1}H NMR spectra were recorded at 400 MHz on a Brüker NMR spectrometer, and chemical shifts are reported in ppm (δ units) downfield from the internal standard TMS. Coupling constants (*J*) are in units of Hertz (Hz). Splitting patterns describe apparent multiplicities and are designated as s (singlet), d (doublet), t (triplet), q (quartet), quint (quintet), m (multiplet), br (broad). Preparative reverse-phase HPLC purification was performed using a SunFire Prep C18 OBD 5 μm 30 x 75 mm column at 35 mL/min. Flash chromatography was performed using Teledyne Isco Combiflash® Rf-200 Companion with normal phase, disposable Redi-Sep flash columns. Mass spectra were obtained on an open access LC-MS system using electrospray ionization. LC conditions: 10% to 80% CH_3CN (0.018% TFA) in 3.0 min with a 1.25 min hold and 0.5 min re-equilibration; detection by MS, UV at 214 nm, and a light scattering detector (ELS). Column: 2.1 X 50 mm Zorbax SB-C8.

Preparation of Compound 2:

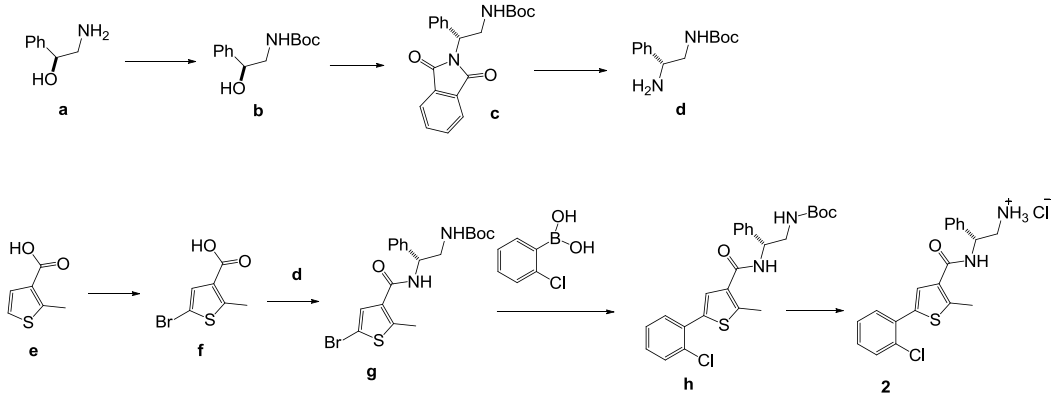

(*S*)-*tert*-butyl (2-hydroxy-2-phenylethyl)carbamate (b). To a solution of **a** (20 g, 146 mmol) in THF (150 mL) at 0 ºC was added Boc_2O (35.5 mL, 153 mmol) in one portion. The mixture was stirred at room temperature for 1 h, and then concentrated *in vacuo*. The residue was suspended in hexane, sonicated for 1 min, and then stirred for 1 h. The solid was collected by filtration and rinsed with hexane (3 times) to afford compound (33 g, 96% yield) as white powder. ^{1}H NMR (400MHz, MeOH-d_4) δ = 7.37 - 7.31 (m, 4H), 7.30 - 7.22 (m, 1H), 4.66 (br. s., 1H), 3.70 (dd, *J*=5.3, 11.4 Hz, 1H), 3.64 (dd, *J*=7.6, 11.4 Hz, 1H), 1.45 (br. s., 9H). LCMS: M+Na^+ = 260.1.

(*R*)-*tert*-butyl (2-(1,3-dioxoisoindolin-2-yl)-1-phenylethyl)carbamate (c). A solution of **b** (10.0 g, 42.1 mmol), isoindoline-1,3-dione (6.20 g, 42.1 mmol) and triphenylphosphine (13.3 g, 50.6 mmol) in THF (200 mL) was placed under an atmosphere of nitrogen, and cooled to 0 ºC.

DEAD (8.01 mL, 50.6 mmol) was added dropwise over 15 min. After the addition was complete, the reaction mixture was stirred at 0 ºC for another 15 min, and then overnight at room temperature. Over this time, a white precipitate formed which was collected by filtration and found to contain both desired product and triphenylphosphine-oxide (Batch 1). The filtrate was concentrated *in vacuo*, and the resulting residue was suspended in 100 mL acetone and sonicated for 5 min. The solids were collected by filtration (Batch 2). Batches 1 and 2 were combined and suspended in 100 mL acetone, heated to 55 ºC for 30 min, cooled to room temperature and then filtered to afford compound **c** (14.1 g, 87% yield) as a white solid. ^{1}H NMR (400MHz, $CDCl_3$) δ = 7.93 - 7.84 (m, 2H), 7.79 - 7.70 (m, 2H), 7.44 - 7.36 (m, 4H), 7.34 - 7.29 (m, 1H), 5.40 - 5.28 (m, 1H), 5.13 (br. s., 1H), 4.06 - 3.87 (m, 2H), 1.27 (br. s., 9H). LCMS: M^++1 = 367; M+Na^+ = 389.3.

(*R*)-*tert*-butyl (2-amino-1-phenylethyl)carbamate (d). To a suspension of (*S*)-tert-butyl (2-(1,3-dioxoisoindolin-2-yl)-1-phenylethyl)carbamate (14.1 g, 38.5 mmol) in EtOH (200 mL) was added hydrazine hydrate (16 mL, 326 mmol), and this mixture was heated to 60 ºC for 3 h. Over this time, a white precipitate formed, and the reaction mixture was cooled to room temperature, filtered, and rinsed with EtOH (50 mL, 3X). The filtrate was then concentrated *in vacuo*, and the resulting residue was diluted with EtOAc (300 mL) and washed with brine (100 mL). The organic layer was dried over Na_2SO_4, filtered, and concentrated. The residue was recrystalized from Et_2O/Hexanes (20 mL/100 mL) to afford compound **d** (6.82 g, 75% yield) as a white solid. ^{1}H NMR (400MHz, DMSO-d_6) δ = 7.37 - 7.18 (m, 5H), 4.40 (q, *J*=7.3 Hz, 1H), 2.71 - 2.60 (m, 2H), 1.37 (s, 9H). LCMS: M^++1 = 237.2.

5-bromo-2-methylthiophene-3-carboxylic acid (f). To a solution of 2-methylthiophene-3-carboxylic acid **(e)** (2 g, 14.07 mmol) in acetic acid (30 mL) was slowly added Br_2 (0.867 mL, 16.88 mmol). The mixture was stirred at 60 °C for 1 h, at which time LCMS showed good conversion to desired product. The reaction mixture was poured into ice water and the resulting precipitate was collected by filtration to afford compound **f** (3.12 g, 12.14 mmol, 86 % yield) as a white solid. ^{1}H NMR (400 MHz, $CDCl_3$) δ ppm 7.33 (s, 1 H), 2.67 (s, 3 H). LCMS: M^++1 = 220.9 / 222.9.

(*R*)-*tert*-butyl (2-(5-bromo-2-methylthiophene-3-carboxamido)-2-phenylethyl)carbamate (g). To a solution of **d** (0.834 g, 3.53 mmol) and **f** (1.0 g, 3.5 mmol) in DMF (10 mL) was added PyBop (2.20 g, 4.23 mmol) and DIPEA (0.92 mL, 5.3 mmol). The mixture was stirred at 25 °C for 2 h. The solvent was removed *in vacuo*, and the resulting residue was purified via automated silica gel chromatography (40 g column, 0-5% MeOH in DCM) to afford compound **g** (1.21 g, 73% yield) as a white solid. ^{1}H NMR (400MHz, MeOH-d_4) δ = 7.42 - 7.34 (m, 5H), 7.32 - 7.25 (m, 1H), 5.12 (dd, *J*=4.9, 9.2 Hz, 1H), 3.51 - 3.41 (m, 1H), 3.41 - 3.35 (m, 1H), 2.58 (s, 3H), 1.44 (s, 9H). LCMS: M^++1 = 439.2 / 441.2.

(*R*)-*tert*-butyl (2-(5-(2-chlorophenyl)-2-methylthiophene-3-carboxamido)-2-phenylethyl)carbamate (h). To a solution of **g** (208 mg, 0.473 mmol) and (2-chlorophenyl) boronic acid (74.0 mg, 0.473 mmol) in 1,4-dioxane (3 mL) and water (1 mL) was added $Pd(PPh_3)_4$ (5.47 mg, 4.73 µmol) and K_2CO_3 (164 mg, 1.18 mmol). The mixture was stirred at 140 °C for 10 min in a microwave reactor. The solvent was evaporated, and the residue was purified via automated silica gel chromatography (24 g column, 0-10% MeOH in DCM) to afford compound **h** (220 mg, 82% yield) as an oil. ^{1}H NMR (MeOH-d_4) δ: 7.67-7.26 (m, 10H), 5.17 (dd, J=8.8, 4.8 Hz, 1H), 3.49 (dd, J=14.4, 9.1 Hz, 1H), 3.41 (dd, J=14.1, 4.8 Hz, 1H), 2.68 (s, 3H), 1.41 (s, 9H). LCMS: M^++1 = 471.2.

(*R*)-*N*-(2-amino-1-phenylethyl)-5-(2-chlorophenyl)-2-methylthiophene-3-carboxamide, hydrochloride (2). To a solution of (*R*)-tert-butyl (2-(5-(2-chlorophenyl)-2-methylthiophene-3-carboxamido)-2-phenylethyl)carbamate (200 mg, 0.352 mmol) in DCM (10 mL) was added TFA (1.0 mL, 13 mmol), and the reaction mixture was stirred at 25 °C for 2 h. The solvent was removed *in vacuo*, and the residue was dissolved in DMSO, and purified by reverse phase HPLC (5-80% MeCN in H_2O and 0.1% TFA, 10 min gradient). The isolated TFA salt was converted to the HCl salt by dissolving in 4 M HCl in dioxane (4.0 mL, 132 mmol), and the mixture was heated at reflux temperature for 2 h. The solvent was evaporated, and this procedure was repeated three times to afford **2** (97 mg, 68% yield) as a white solid. ^{1}H NMR (400 MHz, MeOH-d_4) δ = 7.66 (s, 1 H), 7.64 - 7.59 (m, 1 H), 7.56 - 7.42 (m, 5 H), 7.42 - 7.32 (m, 3 H), 5.45 (dd, *J* = 5.2, 9.7 Hz, 1 H), 3.51 - 3.38 (m, 2 H), 2.69 (s, 3 H). LCMS: M^++1 = 371.2.

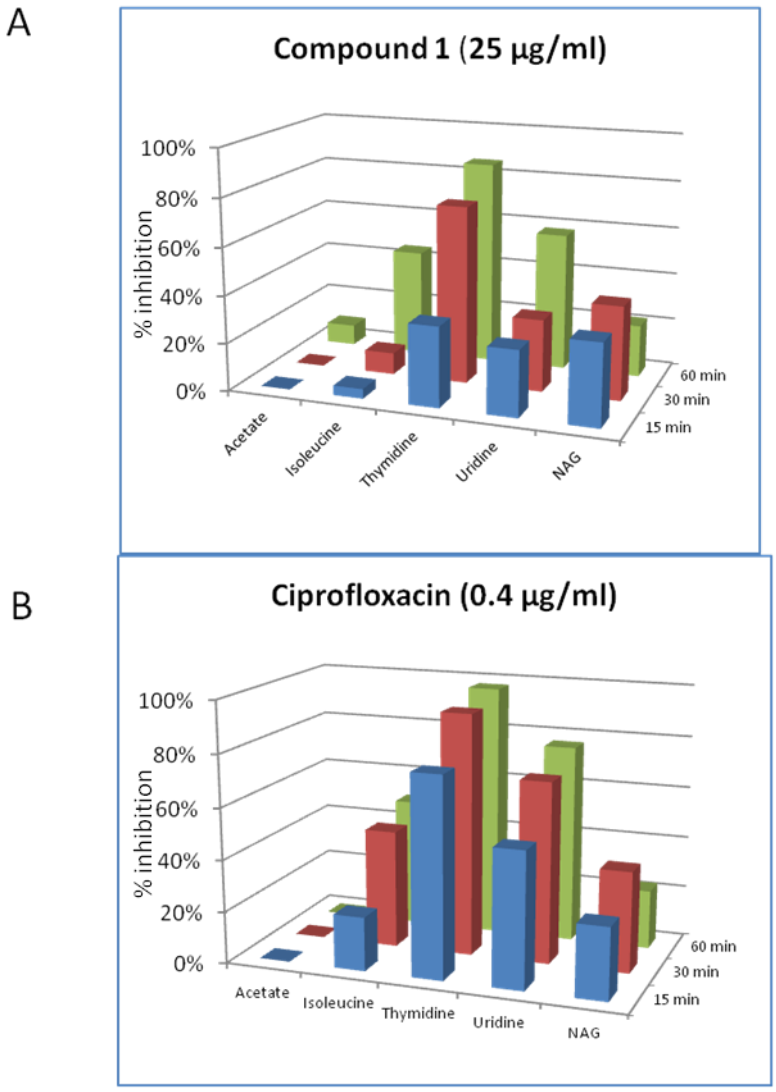

Figure S1. Inhibition of macromolecular synthesis by compound 1 and ciprofloxacin.
E. coli JMZ120 ΔAcrAB (efflux-deficient mutant) was grown to mid-log phase and incubated with inhibitor (**A**) Compound **1** at 25 µg/ml or (**B**) ciprofloxacin at 0.4 µg/ml at 37 °C for 15, 30, and 60 min in the presence of radiolabeled precursors: [^{14}C]-thymidine (at 1 µCi/ml), [^{14}C]-uridine (1 µCi/ml), [^{14}C]-isoleucine (2 µCi/ml), [^{14}C]-acetate (0.5 µCi/ml) or N-acetyl-[^{14}C]-glucosamine (2 µCi/ml) to measure DNA, RNA, protein, fatty acid and cell wall biosynthesis respectively. 10% trichloroacetic acid was added to terminate the reactions, and the cells were harvested using a glass fiber filter plate (PerkinElmer Life Sciences). The filter was dried and counted with scintillation fluid (2). Similar to ciprofloxacin, compound **1** primarily inhibited thymidine incorporation consistent with a DNA replication inhibitor.

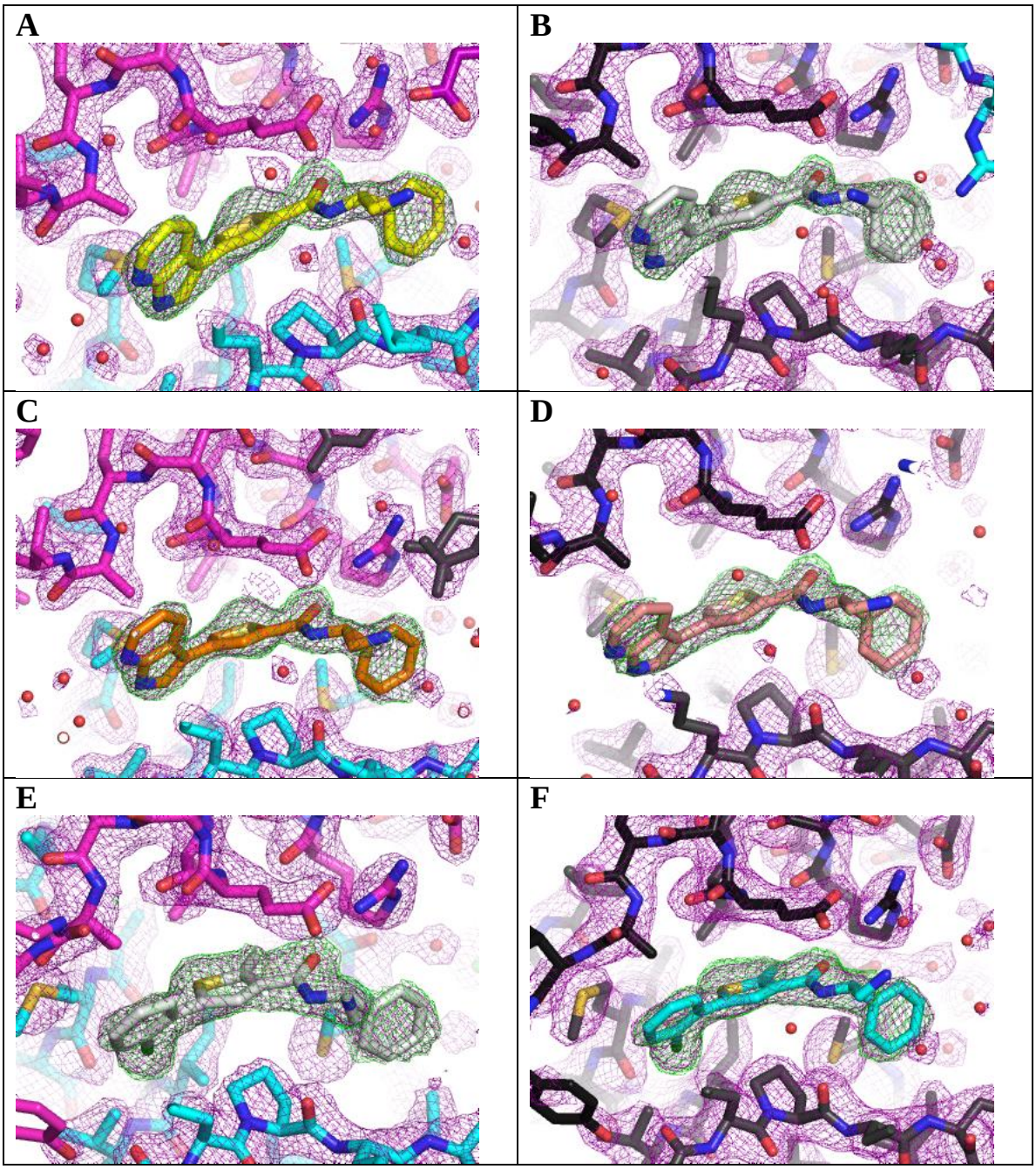

Figure S2. Electron density for thiophene compounds 1 and 2.
(A, B, C, D) Ligand omit map Fo-Fc density (green mesh 3.5 sigma) and final 2Fo-Fc density (purple mesh, 1.3 sigma) for the thiophene **1**, from the four hinge binding pockets from the two complexes in the 1.98Å structure. (**E, F)** Ligand omit map Fo-Fc density (green mesh 3.0 sigma) and final 2Fo-Fc density (purple mesh, 1.1 sigma) for the thiophene **2**, from the two hinge binding pockets in the 2.2Å structure.

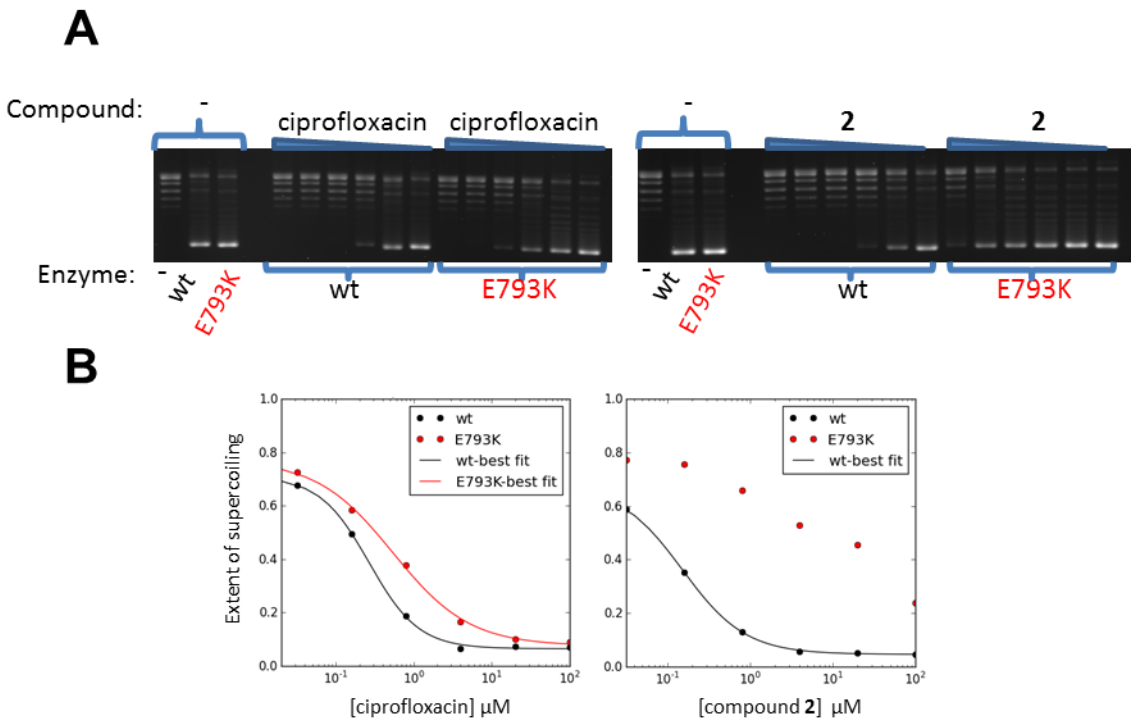

Figure S3. Biochemical evidence that compound 2 uses the same thiophene-binding pocket as compound 1 in *E. coli* DNA gyrase.
(**A**) DNA gyrase-catalyzed supercoiling activity in the presence of ciprofloxacin compared to compound **2** against wild-type (wt) and GyrB-E793K mutant *E. coli* DNA gyrases, following agarose gel electrophoresis. The amount of enzyme is normalized for activity between the wt and the mutant. The extent of supercoiling was measured by the proportion of supercoiled product to the total amount of material in the lane. The compound concentrations are the same for both ciprofloxacin and compound **2**. **(B)** The extent of supercoiling is fitted to a four-parameter logistic curve. – indicates no-compound.

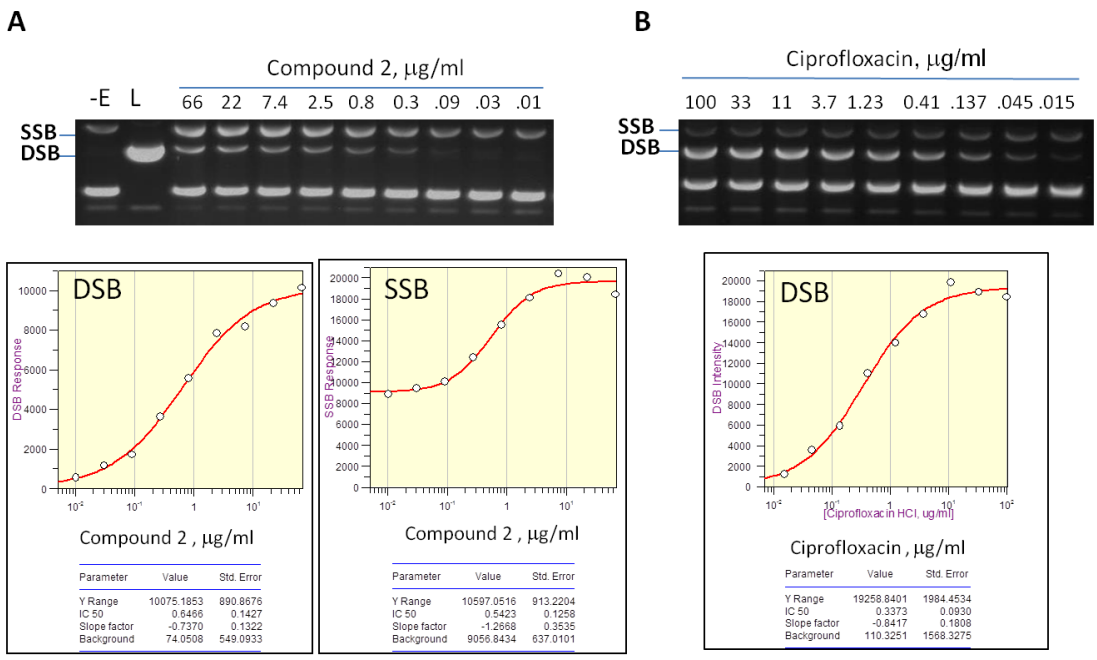

Figure S4. Comparison of stabilization of the cleavage complexes with *E. coli* DNA gyrase by compound 2 and ciprofloxacin.

(**A**) Compound **2** and (**B**) ciprofloxacin at varying concentrations were incubated with supercoiled pBR322 DNA and wild-type *E. coli* DNA gyrase, followed by agarose gel electrophoresis as described in Materials and Methods. The extent of DNA cleavage was determined by measuring the intensities of the DSB and SSB products in the lanes following densitometry, and CC_{50} plotted by fitting the data to a four-parameter logistic curve using GraFit software. Compound **2** stabilizes both DSB and SSB in contrast to ciprofloxacin which mainly stabilizes DSB. DSB=double-stranded DNA breaks (linear DNA), SSB=single-stranded DNA breaks (nicked DNA), – E indicates no DNA gyrase, L= linearized DNA. Table S3 depicts the data from Fig. S4. Also see Fig. 5 and Fig. S5.

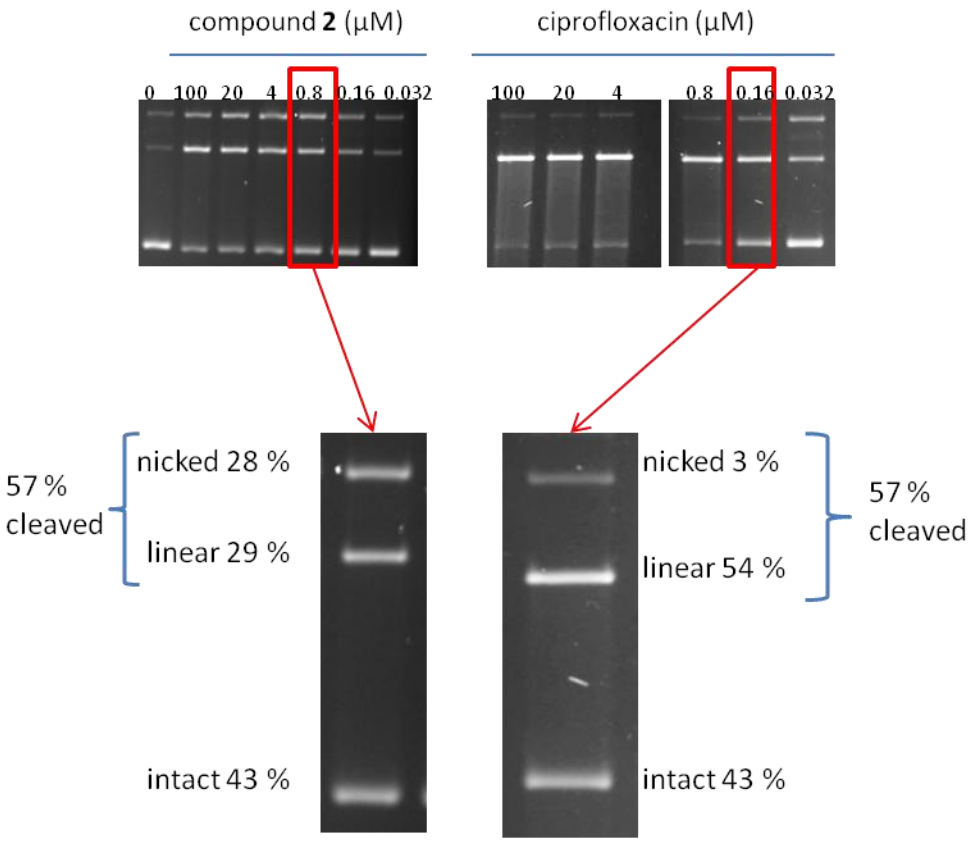

Figure S5.
Compound 2 stabilizes a mixture of double- and single-strand cleavage as opposed to ciprofloxacin, which stabilizes mainly double-strand cleavage.
E. coli DNA gyrase cleavage reactions were performed according to the cleavage assays protocol described by Reece and Maxwell (3). Top left gel depicted is the same as in Figure 5A and shows cleavage induced by compound **2**. The 0.8 µM lane has been singled out (red frame) and enlarged (bottom left). The quantification of each band by density scanning is indicated in terms of percentage of the whole amount of material in the lane. Top right gel depicts a similar experiment performed with the same enzyme stock and concentration and the same substrate incubated with various ciprofloxacin concentrations. The 0.16 µM lane has been singled out (red frame) and enlarged (bottom right). The quantification of each band is indicated as on the left panel. For these two singled out lanes no smearing is apparent (suggesting an absence of multiple cleavage events) and the total extent of cleavage (nicked + linear) is more or less identical. However, compound **2** induces 28% of nicked whereas ciprofloxacin induces only 3%. These data also show that 5 times more compound **2** (0.8 µM) are necessary to induce the amount of total cleavage (nicked + linear) induced by 0.16 µM of ciprofloxacin. Since the IC_{50} of both compounds are comparable (Table S3), this suggests that compound **2** and ciprofloxacin have comparable potency in forming inhibitory ternary complexes, whereas a higher proportion of those are fully cleaved in the case of ciprofloxacin. We therefore suggest the existence of compound **2**-gyrase-DNA ternary complexes that block the enzyme but do not result in cleavage when trapped with SDS.

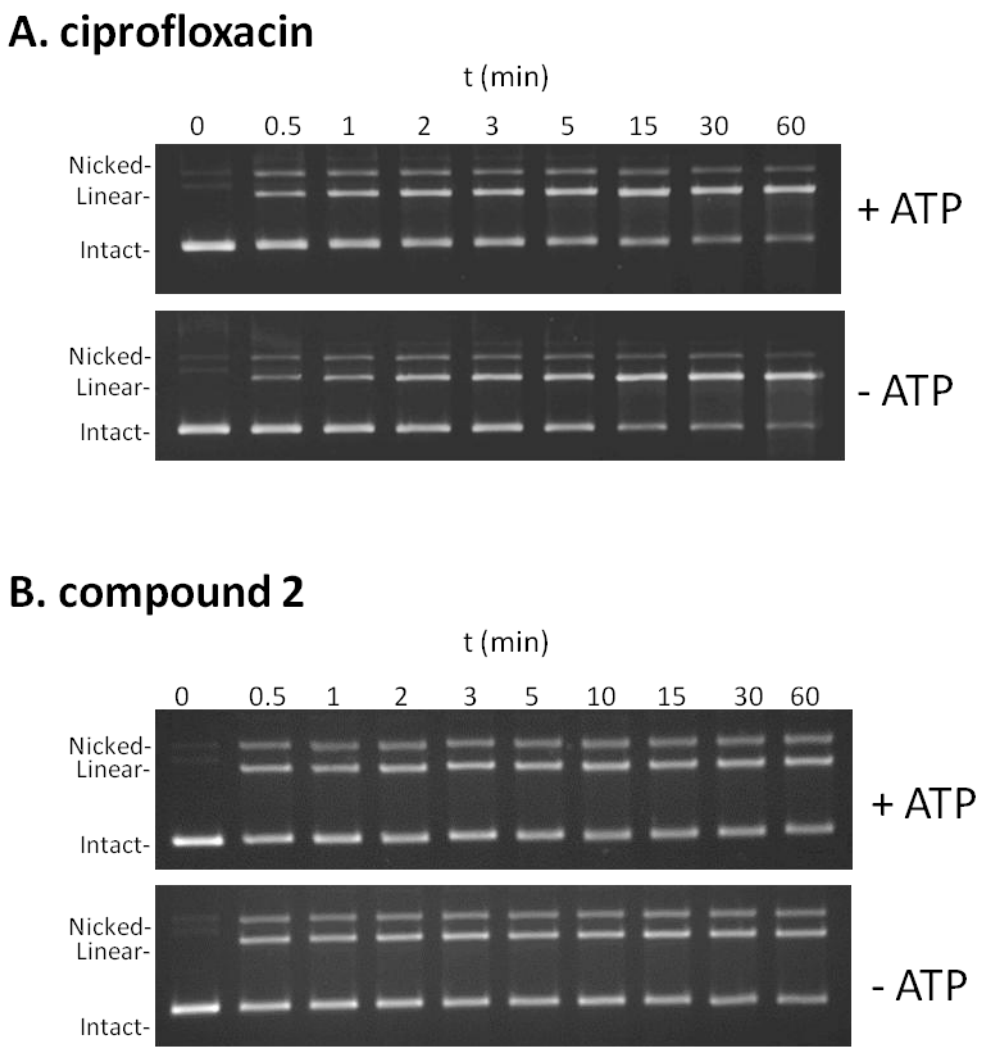

Figure S6. Kinetics of cleavage.

E. coli DNA gyrase cleavage reactions were performed according to the cleavage assays protocol described by Reece and Maxwell (3) but with different incubation times, as indicated. The reactions are started by addition of the enzyme (~ 0.1 µg of A_2B_2 for each reaction) and stopped by SDS trapping (addition of SDS to 0.2% w/v). For the 0 minute time point the enzyme and SDS are mixed in simultaneously by deposition of each reagent on the side of the tube and vortexing. (**A)** Reactions performed in the presence of 4 µM of ciprofloxacin either in the presence (top) or the absence (bottom) of 1 mM ATP, which slightly increases the rate of appearance of ciprofloxacin-induced cleavage (compare both conditions for time 0.5, 1, and 2 minutes). (**B)** Reactions performed in the presence of 4 µM of compound **2** either in the presence (top) or absence (bottom) of 1 mM ATP. No detectable difference is observed. The minus ATP conditions were quantified for both compounds by density scanning of each band and plotted in Figure 6. With this enzyme dose, no significant smearing due to multiple cleavage events is observed in any condition except at 60 minutes with ciprofloxacin. This leads to a slight underestimation of the final amount of cleavage but it does not affect the main conclusion from these data, because the differences are visible mainly for the earlier time points, where no smearing occurs.

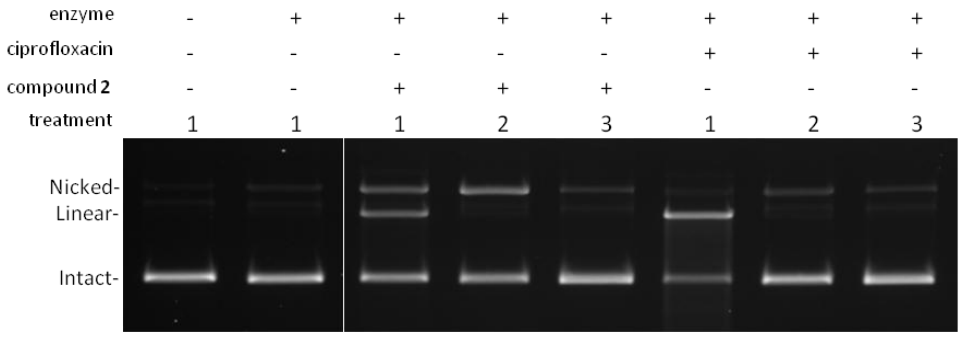

Figure S7. Reversal of cleavage complexes stabilized by ciprofloxacin and compound 2.
E. coli DNA gyrase cleavage reactions on relaxed pBR322 were performed according to the protocol described by Reece and Maxwell (3) and run on an ethidium bromide gel after different post-incubation treatments. Treatment 1 consists of SDS trapping of cleavage complexes (addition of SDS to a final concentration of 0.2% w/v) followed by digestion with 20 µg of proteinase K. Treatment 2 consists of addition of EDTA pH 8.0 at 8 mM final, followed by incubating 30 minutes at room temperature. SDS trapping is then performed as in treatment 1. Treatment 3 consists of addition of EDTA at 8 mM, followed by incubating 30 minutes at room temperature. Subsequently, the sample is digested with 20 µg of proteinase K. No SDS is added at any point for this treatment. Treatment 3 results in the complete reversal of cleavage stabilized by either compound 2 or ciprofloxacin. It is therefore used to analyze the topology of cleavage complexes (see main text and Figure 7).

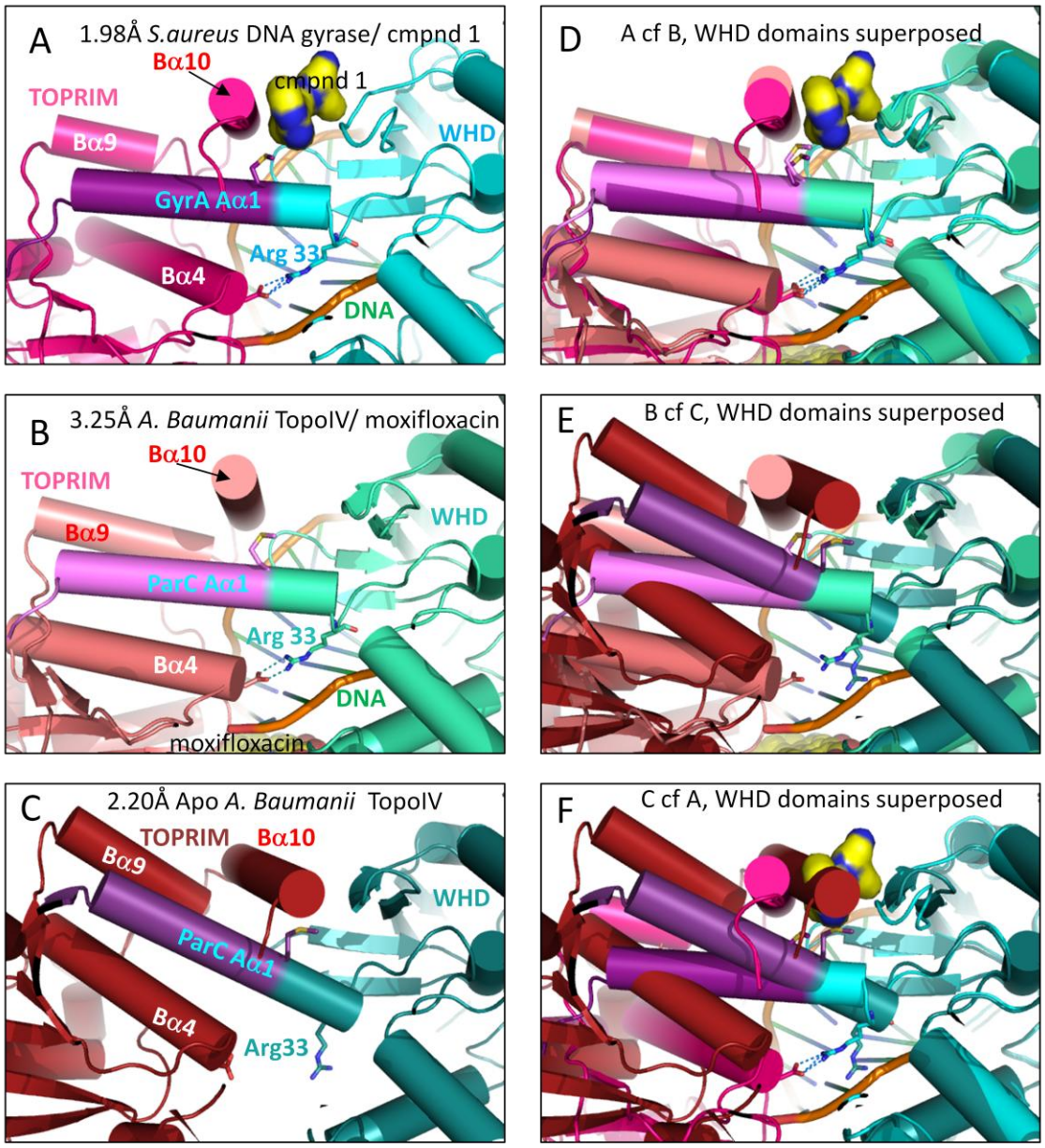

Figure S8. Movement around the bacterial Aα1 hinge can close the compound binding pocket.

(**A**) View of 1.98Å crystal of *S. aureus* DNA gyrase with compound **1**. (**B**) View of 3.25Å crystal structure of *A. baumannii* topoIV with moxifloxacin (pdb code 2XKK). (**C**) View of the 2.2Å Apo *A. baumannii* topoIV structure (pdb code 2XKJ). (**D**) Comparison of 1.98Å crystal of *S. aureus* DNA gyrase with compound **1** and 3.25Å crystal structure of *A. baumannii* topoIV with moxifloxacin. (**E**) Comparison of the two *A. baumannii* structures (see also supplementary Fig. 3 from Wohlkonig et al. (4)). (**F**) The 2.20Å Apo *A. baumannii* topoIV structure compared to the 1.98Å crystal of S. *aureus* DNA gyrase with compound **1**. Note the relative movement of the Bα10 helix.

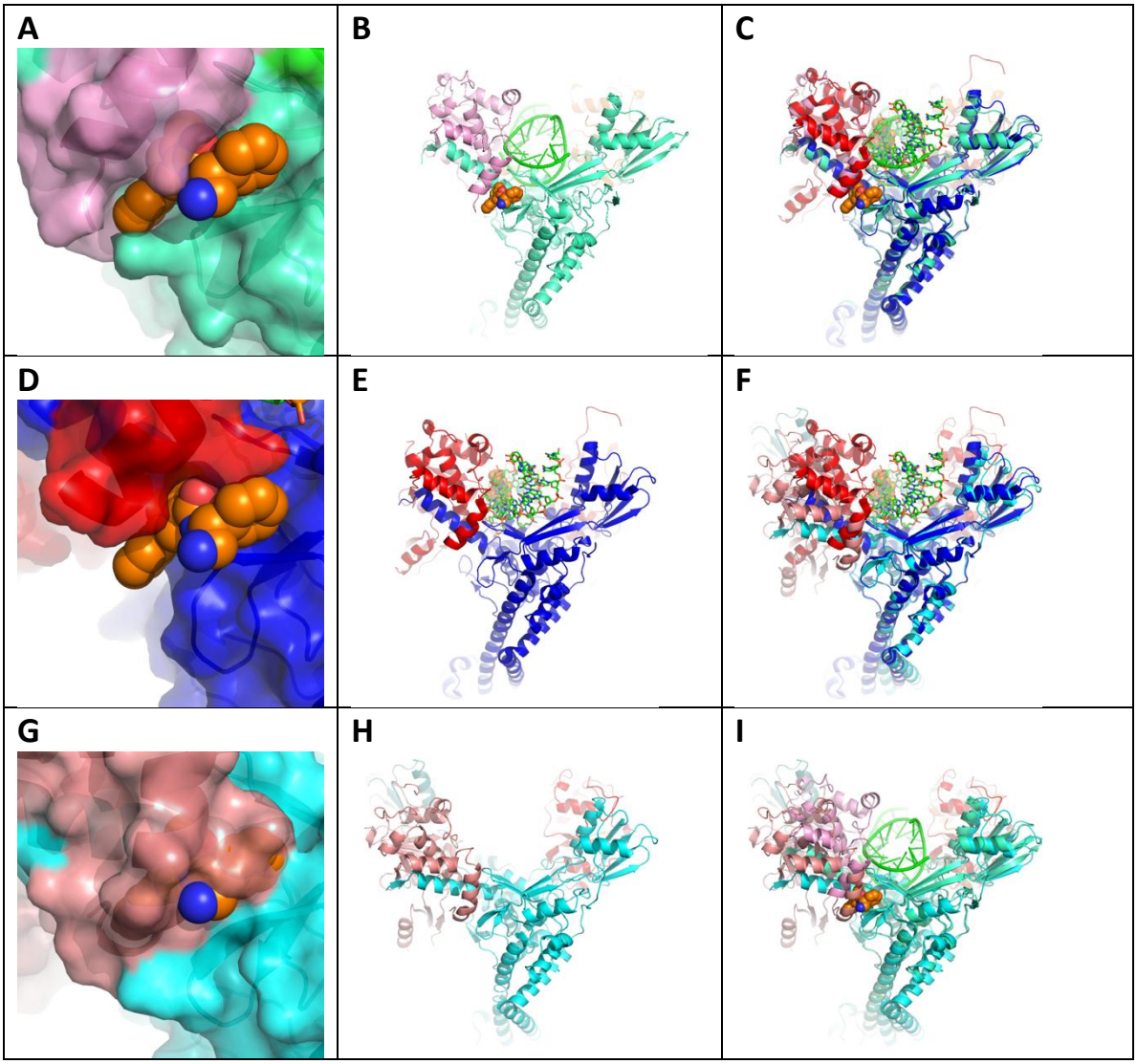

Figure S9. The Aα1-hinge pocket is present in an *A. baumannii* topo IV complex with DNA and moxifloxacin, but is not present in an Apo *A. baumannii* crystal structure. (**A, B**) Two views of the complex of thiophene compound **2** with *S. aureus* DNA gyrase and DNA. (**C**) The crystal structure of an *A. baumannii* topoisomerase IV complex with DNA and moxifloxacin (pdb code: 2xkk) is shown superposed on the *S. aureus* thiophene complex. (**D, E**) Two views of the moxifloxacin complex with DNA and *A. baumannii* topo IV. In D, thiophene **2** is also shown based on the superposition in panel C. (**F**) Superposition of the apo *A. baumannii* structure (2xkj) and the complex with moxifloxacin (2xkk). The ParC (blue/cyan) subunits have had their WHD domains superposed. Note the movement of the TOPRIM domains (4). (**G, H**) Two views of the apo *A. baumannii* topo IV structure (2xkj). In G, thiophene **2** is also shown based on the superposition in panel I. Note that the pocket for the thiophene is not present in this apo structure due to relative domain movements. (**I**) Superposition of the apo *A. baumannii* structure (2xkj) and the complex of thiophene **2** with *S. aureus* DNA gyrase and DNA.

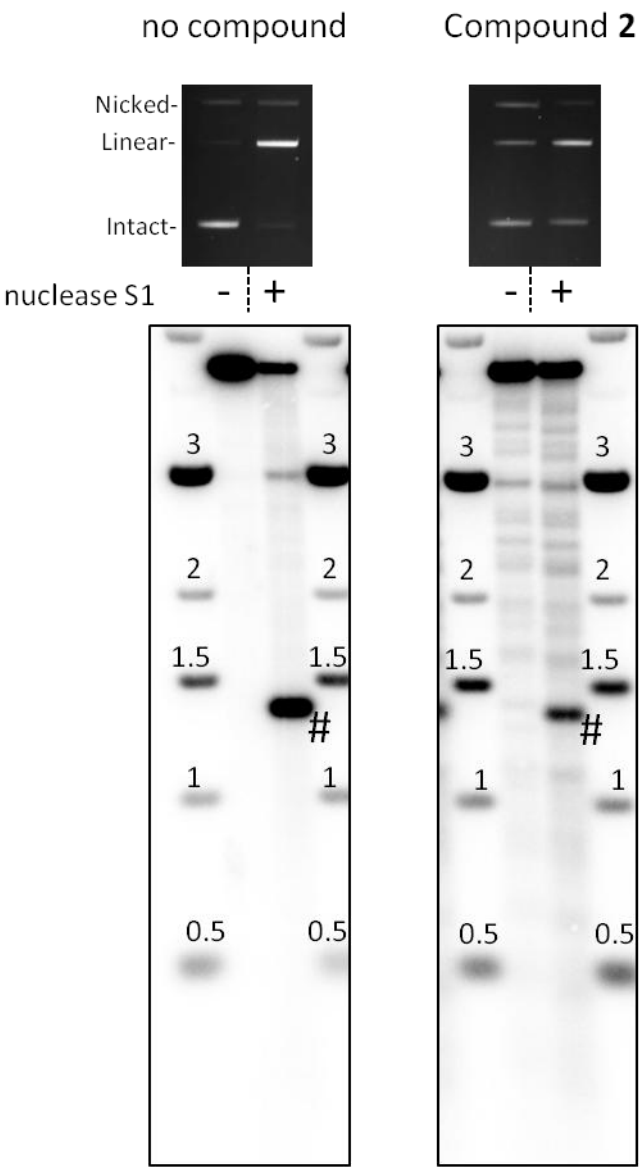

Figure S10. Mapping of nuclease S1 digested, compound 2-induced cleavage.

E. coli DNA gyrase cleavage reactions were performed according to the cleavage assays protocol described by Reece and Maxwell (3) and were either digested with nuclease S1 or mock-digested. A small aliquot of each is analyzed on an ethidium bromide agarose gel (Top panels and Materials and Methods). The rest of the reactions are digested by *Eco*R1, analyzed by agarose gel electrophoresis and the DNA transferred to a nitrocellulose membrane and hybridized with a small PCR fragment (Bottom panels and Materials and Methods). A DNA ladder was loaded alongside (sizes are indicated next to each band in kbp). #: This band is strictly dependent on prior digestion with nuclease S1 and strongest in the "no compound" reactions (see bottom panels). Moreover, the S1 nuclease converts a significant amount of uncleaved DNA into linear only in the "no compounds" reactions. We therefore interpret this band as reflecting the digestion by nuclease S1 of a DNA hairpin. In addition, since the initial plasmid substrate is relaxed, the inhibition of gyrase activity by compound **2** prevents the introduction of negative superhelicity and thereby limits the formation of the hairpin, explaining why band # is weaker when compound **2** is present.

Table S1. X-ray data collection and refinement statistics.

	Compound 1* (co-crystal) PDB code: 5NPK	**Compound 2** (soak into GSK945237 co-crystal) PDB code: 5NPP
Data collection		
Beamline	DLS I02	DLS I04-1
Space group	$P2_1$	$P6_1$
Cell dimensions a,b,c (Å) α, β, γ (°)	89.4, 120.7, 168.9 90.0, 90.0, 90.0	92.9, 92.9, 410.0 90.0, 90.0, 120.0
Wavelength (Å)	0.9795	0.9173
Resolution range (Å)	20.0-1.98 (2.01-1.98)	20.0-2.22 (2.26-2.22)
No. of unique reflections	245600 (10975)	97193 (4830)
Multiplicity	3.6 (2.5)	5.2 (4.9)
Completeness (%)	98.7 (94.5)	99.1 (99.3)
R_{merge} (%)	6.9 (67.3)	11.1 (115.8)
I/σI	11.8 (1.5)	9.5 (1.1)
CC (1/2)	0.998 (0.542)	0.997 (0.538)
Refinement		
Resolution (Å)	20.0-1.98 (2.03-1.98)	20.0-2.22 (2.27-2.22)
No. reflections	245569 (15099)	97193 (7127)
R_{work}/ R_{free} (%)	15.7/18.5 (25.7/28.0)	18.4/22.7 (32.1/33.2)
No. Atoms		
Protein	22195	10936
DNA	1803	941
Ligand/ion	304	170
Water	2682	846
B-factors		
Protein	19	42
DNA	39	45
Ligand/ion	47	49
Water	46	47
R.m.s deviations		
Bond lengths (Å)	0.013	0.015
Bond angles (°)	1.661	1.727

* The compound **1** structure is twinned (refined twin fractions - 0.76/0.24).

Table S2. Amino acid alignments of thiophene-binding pocket shows it is well conserved in key pathogens.

	GyrB 630	637	GyrA 27 30	179	343
S.aur	VENR**R**QF**IE**DN**A**VY		FLDYA**M**SV**I**VARALP	ASGIAVG**M**ATNIPP	G-R**P**KLI
Str.pn	VEPR**R**EF**IE**EN**A**VY		FIDYA**M**SV**I**VARALP	ATGIAVG**M**ATNIPP	G-I**P**KIL
H.flu	VEPR**R**EF**IE**LN**A**LR		YLDYA**M**SV**I**VGRALP	SSGIAVG**M**ATNIPP	G-Q**P**RLF
E.coli	VEPR**R**AF**IE**EN**A**LK		YLDYA**M**SV**I**VGRALP	SSGIAVG**M**ATNIPP	G-Q**P**KIM
E.aero	VEPR**R**AF**IE**EN**A**LK		YLDYA**M**SV**I**VGRALP	SSGIAVG**M**ATNIPP	G-Q**P**KIM
E.cloa	VEPR**R**AF**IE**EN**A**LK		YLDYA**M**SV**I**VGRALP	SSGIAVG**M**ATNIPP	G-Q**P**KIM
K.pneu	VEPR**R**AF**IE**EN**A**LK		YLDYA**M**SV**I**VGRALP	ASGIAVG**M**ATNIPP	G-Q**P**KIM
P.mira	VEPR**R**AF**IE**EN**A**LK		YLDYA**M**SV**I**VGRALP	SSGIAVG**M**ATNIPP	G-Q**P**KLL
P.aer	VEPR**R**DF**IE**SN**A**LK		YLDYA**M**SV**I**VGRALP	SSGIAVG**M**ATNIPP	G-Q**P**RTL
A.bau	VEPR**R**AF**IE**EN**A**LN		YLDYA**M**SV**I**VSRALP	AAGIAVG**M**ATNMAP	G-Q**P**KLM
M.tb	VDAR**R**SF**I**T**R**N**A**KD		YIDYA**M**SV**I**VGRALP	SGGIAVG**M**ATNIPP	G-V**P**RTL

	ParE		ParC		
S.aur	VQPR**R**EW**IE**KH**V**EF		FGRYS**K**YI**I**QERALP	STGISAG**Y**ATDIPP	G-R**P**KLM
Str.pn	VEPR**R**KW**IE**DN**V**KF		FGRYS**K**YI**I**QERALP	STGISSG**Y**ATDIPP	G-R**P**KLM
H.flu	SEDR**K**NW**LQ**AK**G**DQ		YLNYS**M**YV**I**MDRALP	TTGIAVG**M**ATDIPP	DHK**P**AVK
E.coli	SEDR**R**NW**LQ**EK**G**DM		YLNYS**M**YV**I**MDRALP	TTGIAVG**M**ATDIPP	DGR**P**AVK
E.aero	SEDR**R**NW**LQ**EK**G**DM		YLNYS**M**YV**I**MDRALP	TTGIAVG**M**ATDIPP	DNR**P**AVK
E.cloa	SEDR**R**NW**LQ**EK**G**DM		YLNYS**M**YV**I**MDRALP	TTGIAVG**M**ATDIPP	DGR**P**ASK
K.pneu	SEDR**R**NW**LQ**EK**G**DM		YLNYS**M**YV**I**MDRALP	TTGIAVG**M**ATDIPP	DGR**P**AVK
P.mira	SEDR**R**NW**LQ**EK**G**DE		YLNYS**M**YV**I**MDRALP	TTGIAVG**M**ATDIPP	DNR**P**AVK
P.aer	AGDR**K**SW**LE**SK**G**NL		YLNYS**M**YV**I**MDRALP	TTGIAVG**M**ATDVPP	DGK**P**QVK
A.bau	AADR**K**QW**LE**QK**G**NL		YLNYA**M**YV**I**MDRALP	TTGIAVG**M**ATDIPP	DGR**P**QVK

	TOP2A				
Human	IDDR**K**EW**L**T**N**F**M**ED		LILFS**N**SD**N**E-RSIP	AEGIGTG**W**SCKIPN	VGC**L**KKY
	TOP2B				
Human	IDDR**K**EW**L**T**N**F**M**ED		LILFS**N**SD**N**E-RSIP	AEGIGTG**W**ACKLPN	MGC**L**KKY

Residues in bold are the eight main residues that form the thiophene binding pocket as detected in the co-crystal structure (*S. aureus* residues shown in red, *S. aureus* residue numbering). Residues in blue highlight the differences of ParC/E residues from the conserved binding residues of GyrA/B; note also that *M.tb* Gyrase also has one difference. Sequences are from three Gram-positive pathogens: S.aur, *Staphylococcus aureus*; Str.pn, *Streptococcus pneumonia*e; M.tb, *Mycobacterium tuberculosis*, and eight Gram-negative pathogens: H.flu, *Haemophilus influenza*e; E.coli, *Escherichia coli*; E.aero, *Enterobacter aerogenes*; E.cloa *Enterobacter cloacae*, K.pneu, *Klebsiella pneumonia*e; P.mira, *Proteus mirabilis*; P.aer, *Pseudomonas aeruginosa*; A.bau, *Acinetobacter baumannii*. Also shown are sequences from the two human type IIA topoisomerases. Note that *M.tb* does not have a topoisomerase IV.

Table S3. Target activity of thiophene inhibitors.

Assay	Enzyme activity, μg/ml (μM)		
	Compound **1**	Compound **2**	Ciprofloxacin
E. coli DNA gyrase supercoiling IC_{50}	5 (13.8)	0.1 (0.3)	0.2 (0.6)
E. coli DNA gyrase cleavage CC_{50}	11.4 (31.5)	0.6 (1.6)	0.3 (0.9)
E. coli topo IV decatenation IC_{50}	> 50 (>140)	> 200 (>540)	1.9 (5.7)

Cleaved-complex CC_{50} is the concentration of compound needed to induce 50% of maximal double-strand DNA breaks. For representative DNA gyrase cleavage gels, see Fig. S4. For DNA gyrase supercoiling assays, a representative IC_{50} plot of compound **1** is shown below that corresponds to the gel scan depicted in Fig.1A. The IC_{50} is reported as an average of independent experiments in Table S3. Data is shown in both μg/ml and μM (in brackets).

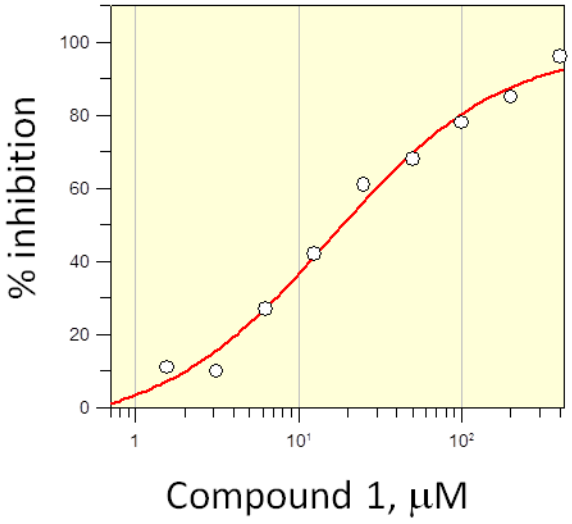

Parameter	Value	Std. Error
Y Range	105.6144	20.8548
IC 50	15.7501	4.8850
Slope factor	-0.8252	0.2728
Background	-6.4067	13.9418

Table S4. Cross resistance of compounds 1 and 2 to thiophene-resistant gyrase mutants confirm compounds antibacterial mode-of-action.

Bacterial strain	Mutation	MIC (μg/ml)		
		Thiophene compound		Quinolone
		1	**2**	**Ciprofloxacin**
E. coli TOP10 Δ*tolC*[a]	wt	4	0.063	0.0005
	GyrB E793K	16	2	0.0005
	GyrB E793G	16	2	0.0005
	GyrA L34Q	16	1	0.002
	GyrA G173S	32	1	0.001
	GyrA V176A	16	2	0.002
E. coli TOP10[c]	wt	NT	8	0.002
	GyrB R789C	NT	32	0.004
	GyrA A175V	NT	32	0.008
	GyrA A175T	NT	32	0.008
	GyrA V28A	NT	32	0.004
	GyrA A33T	NT	64	0.004
E. coli 7623[c]	wt	NT	8	0.004
	GyrA A25V	NT	>64	0.004
	GyrA P342L	NT	>64	0.004
A. baumannii BM4454[b]	wt	NT	4	64
	GyrB R808C	NT	64	64
	GyrA P33S	NT	32	64
	GyrA Q92P	NT	32	32
	GyrA P263L	NT	32	64
A. baumannii BM4652 Δ*adeABC* Δ*adeIJK*[d]	wt	8	0.25	1
	GyrA A23V	16	8	1
	GyrA G171S	16	NT	1
K. pneumoniae JH1 Δ*tolC*[d]	wt	8	0.25	0.008
	GyrA A25V	8	16	0.004

Laboratory-generated resistant mutants were selected to compounds **1**[a], **2**[b] and close analogs [c, d]. Note: *A.baumannii* GyrB R808 residue is equivalent to *E.coli* GyrB R789 in the thiophene-binding pocket, wt = wild-type.

References

1. Seefeld MA, *et al.* (2009) Discovery of 5-pyrrolopyridinyl-2-thiophenecarboxamides as potent AKT kinase inhibitors. *Bioorg. Med. Chem. Lett.* 19(8):2244-2248.
2. King AC & Wu L (2009) Macromolecular synthesis and membrane perturbation assays for mechanism of action studies of antimicrobial agents. *Curr. Protoc. Pharmacol* 47(13A):7.1-7.23.
3. Reece, R.J. and Maxwell, A. (1989) Tryptic fragments of the *Escherichia coli* DNA gyrase A protein. *The Journal of biological chemistry*, **264**, 19648-19653.
4. Wohlkonig A, *et al.* (2010) Structural basis of quinolone inhibition of type IIA topoisomerases and target-mediated resistance. *Nat. Struct. Mol. Biol* 17(9):1152-1153.